



with the expansion of allergen-specific Foxp3<sup>+</sup> Treg cells, suggesting that the suppressive effect was mediated by Foxp3<sup>+</sup> Treg cells. Moreover the protective effect of H3N1 infection could be replicated by treating suckling mice with NKT cell-activating glycolipids from *H. pylori* or with  $\alpha$ -C-GalCer. These studies are particularly important not only because they characterize an NKT cell population that suppresses AHR, but also because they provide a plausible mechanism for the hygiene hypothesis and for epidemiological studies indicating that infection with respiratory viruses (9) and *H. pylori* (2, 3) protect against the development of asthma.

NKT cells comprise a small subset of T lymphocytes that share characteristics with NK cells and conventional T cells, with potent functions in modulating immunity that have only recently become appreciated (33). NKT cells express a relatively unique transcription factor, PLZF, specific for NKT cells (34) and other innate or activated T cells (35), and an invariant TCR, V $\alpha$ 14J $\alpha$ 18 in mice and V $\alpha$ 24 in humans, and are restricted by the MHC class I-like molecule, CD1d. The conservation of this invariant TCR across many mammalian species suggests that it is a pattern recognition receptor, and that NKT cells play an important role in innate immunity. Activation of NKT cells through this invariant TCR results in the rapid production of large amounts of cytokines, including IL-4 and IFN- $\gamma$ , particularly from mature NKT cells found in adult mice and humans. In contrast, NKT cells in neonates or in cord blood are immature, and produce only small amounts of cytokines (36, 37). Nevertheless, the ability of mature NKT cells to rapidly produce very large quantities of cytokines endows that NKT cell with the capacity to play very important regulatory roles in autoimmunity, cancer, asthma, and infectious diseases (38).

NKT cells participate in immune responses to a growing list of infectious microorganisms, driven either by direct TCR recognition of specific glycolipids expressed by microorganisms, as in the case of *Borrelia burgdorferi* (39) and *Sphingomonas paucimobilis* (32, 40), or by indirect responses to cytokines released by activated DCs, as in the case of *Salmonella typhimurium* (41), *E. coli*, *Staphylococcus aureus*, *Listeria monocytogenes* (42), and *Mycobacteria tuberculosis* (43, 44). During influenza A infection in adult mice, NKT cells abolished the suppressive activity of influenza A-induced myeloid-derived suppressor cells, thereby enhancing survival (18). Our current studies also suggest that NKT cells may respond during infection with influenza A, and to glycolipids (PI57) produced by *H. pylori*, resulting in inhibitory effects on immunity, though primarily in young mice. The capacity of *H. pylori* glycolipids to activate a regulatory NKT cell subset (but only in young mice) may also explain the protective effects of *H. pylori* infection in neonatal but not older mice against gastritis and malignant metaplasia (45) as well as the observation that only WT, and not cholesterol- $\alpha$ -glucosyltransferase-deficient, *H. pylori* can infect the gastric mucosa of mice (28), given that cholesterol- $\alpha$ -glucosyltransferase is required for synthesis of PI57 (46). Finally, we would like to point out that the structure and function of PI57 is unique, since it includes a cholesterol-containing tail distinct from previously described NKT cell ligands, and since it represents the first demonstration of cholesterol as a target for TCR recognition.

NKT cells thus react to a diverse group of pathogens by functioning as an innate immune cell that can sense and rapidly respond to the presence of infectious agents. The capacity to respond to such pathogens, however, may be limited in neonates and young children due to limited numbers and to the immaturity of NKT cells (36, 37). On the other hand, the immaturity of NKT cells in young

children may provide an opportunity for infection and therapeutic intervention to influence the subset composition of NKT cells, thereby preventing the development of asthma and allergy.

In asthma, NKT cells have been suggested to play a very important pathogenic role (20, 47). This idea has become controversial, since some patients, particularly those with mild or well-controlled asthma, have few detectable pulmonary NKT cells, although patients with severe or poorly controlled asthma have a significant increase in pulmonary NKT cells (19, 48, 49). Nevertheless, in many distinct mouse models of asthma, the presence of specific NKT cell subsets was required for the development of AHR. For example, CD4<sup>+</sup>IL-17RB<sup>+</sup> NKT cells are required in allergen-induced AHR (19, 20, 50, 51); in ozone-induced AHR, an NK1.1<sup>-</sup>IL-17-producing subset is required (21); and in Sendai virus-induced AHR, a CD4<sup>+</sup> NKT cell population that interacts with alternatively activated alveolar macrophages is required (22). While previous studies have suggested that some (DN) NKT cells could not induce AHR (50), we now show for the first time that a population of NKT cells, enriched for a DN, T-bet-dependent, and IFN- $\gamma$ -producing subset, has a potent regulatory role, suppressing the development of AHR. Although previous studies have suggested an inhibitory role for NKT cells in asthma, since adoptive transfer of NKT cells acutely activated with  $\alpha$ -GalCer (1 hour prior to transfer) inhibit the development of experimental asthma in a C57BL/6 mouse model (52), we believe that our current studies are quite distinct. We showed that H3N1 infection in suckling mice expanded a population of NKT cells that, when examined 42 days after infection, specifically suppressed allergen-induced AHR without the need for acute activation with exogenous glycolipids.

While H3N1 infection affects many different cell types, the fact that the protective effect of H3N1 infection could be transferred with purified NKT cells, and the fact that the protective effect could be replicated by treatment of suckling mice with  $\alpha$ -C-GalCer or a glycolipid from *H. pylori* (PI57) that specifically activated NKT cells in a CD1d-restricted fashion, strongly suggests that the protective effect of H3N1 infection in young mice was primarily mediated by a subset of NKT cells. The NKT cell subset activated by PI57 in suckling mice appeared to be a subset of invariant NKT cells, since DN NKT cells in suckling mice expanded after treatment with PI57, and since CD1d tetramers loaded with PI57 could stain NKT cells. The precise mechanism by which the DN NKT cells suppressed AHR is not clear, but may involve the preferential production of IFN- $\gamma$  but not IL-4, since DN NKT cells from H3N1-infected suckling *Tbet*<sup>-/-</sup> mice failed to inhibit AHR. A role for IFN- $\gamma$  is also supported by our observation that treatment of suckling mice with  $\alpha$ -C-GalCer, which preferentially induces IFN- $\gamma$  (26), also prevented the development of OVA-induced AHR 42 days later, whereas treatment with  $\alpha$ -GalCer or with *Sphingomonas* glycolipid (PBS30) did not.

The "regulatory" NKT cells mediating the inhibitory effect of H3N1 and of PI57 and  $\alpha$ -C-GalCer may be similar to previously described DN NKT cells that protected against the development of type I diabetes in humans and in mice (53, 54), to IFN- $\gamma$ -producing NKT cells that were required for allograft tolerance (55), or to IL-4-producing NKT cells that induced Treg cells in the prevention of graft versus host disease (56–58). In our experiments, increased numbers of both natural and adaptive OVA-specific Treg cells were associated with the regulatory NKT cells and were blocked by treatment with anti-CD25 mAb (Figure 4, F and G). Moreover, we believe that our studies are the first to demonstrate the existence of a

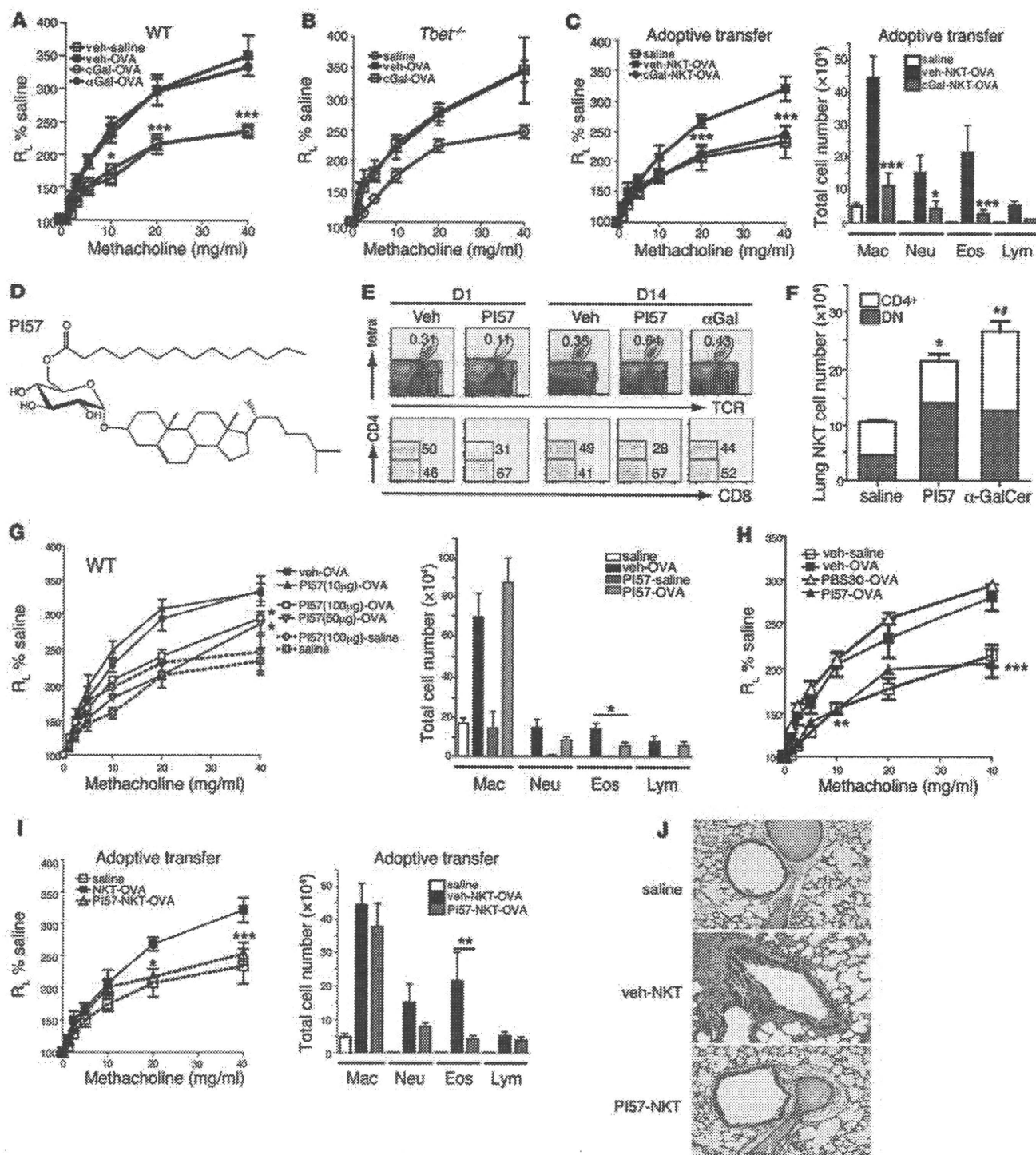


**Figure 6**

Induction of protection with  $\alpha$ -C-GalCer and a glycolipid from *H. pylori*. (A) Two-week-old BALB/c mice ( $n = 6-8$ /group) or (B) *Tbet*<sup>-/-</sup> mice ( $n = 4-6$  per group) received 5  $\mu$ g  $\alpha$ -GalCer (cGal), 2  $\mu$ g  $\alpha$ -GalCer, or vehicle. After OVA sensitization and challenge, AHR was measured on day 44. (C) Donor mice were treated with  $\alpha$ -C-GalCer (5  $\mu$ g) or vehicle i.p. NKT cells served as donors, as in Figure 4A ( $n = 4$  per group). Lung resistance (left) and cell counts in BAL (right) were assessed. (D) Structure of PI57. (E) Mice received PI57 (50  $\mu$ g),  $\alpha$ -GalCer (2  $\mu$ g), or vehicle i.p., and lungs were examined 1 or 14 days later for CD4 and CD8 expression. (F) Absolute numbers of CD4<sup>+</sup> NKT and DN NKT subsets from E were assessed. (G) BALB/c mice ( $n = 5-8$ /group) received PI57 or vehicle i.p. Lung resistance (left) and BAL cells (right) were assessed. (H) BALB/c mice treated with PI57 (50  $\mu$ g), PBS30 (*Sphingomonas* glycolipid) (50  $\mu$ g), or vehicle i.p. were assessed for AHR as in G. (I) Donor mice were treated with PI57 (50  $\mu$ g) or vehicle i.p. NKT cells served as donors as in Figure 4A. Lung resistance (left) and BAL cells (right) were assessed ( $n = 4$  per group). (J) Representative lung sections from I stained with H&E (original magnification,  $\times 10$ ). Data represent 2-3 independent experiments. \* $P < 0.05$ , \*\* $P < 0.05$ , \*\*\* $P < 0.001$  versus vehicle-OVA (C, G, and I), DN NKT saline (F), and CD4<sup>+</sup> NKT saline (F).

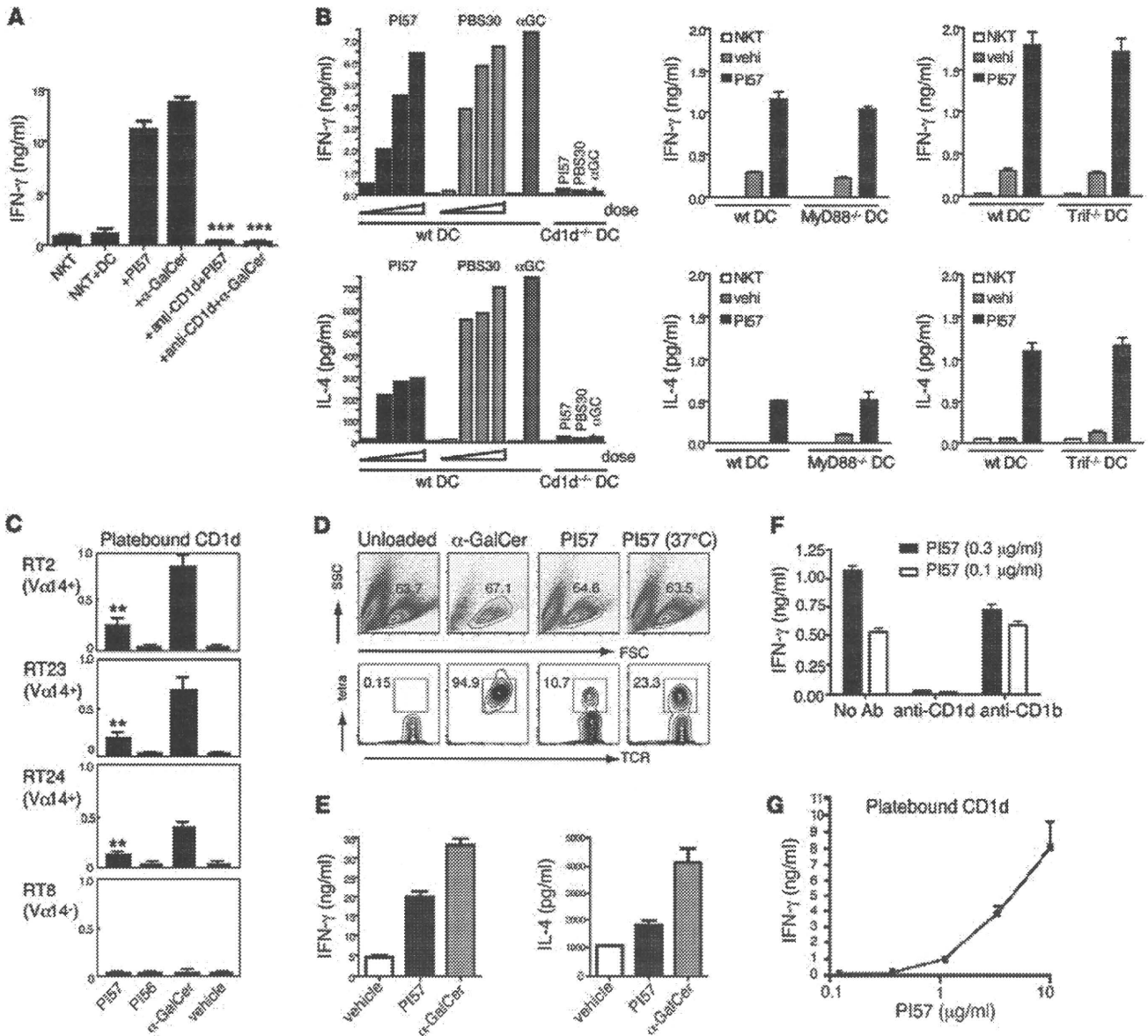


**Figure 7**

PI57 directly activates NKT cells. (A) NKT cell lines were cocultured with BM-derived DCs (BMDCs) and α-GalCer (100 ng/ml), PI57 (10 μg/ml), or vehicle for 48 hours, with or without pre-incubation with anti-CD1d (10 μg/ml). IFN-γ was measured by ELISA. (B) Murine NKT cell lines were cocultured as in A with BMDCs from WT, *Cd1d*<sup>+/+</sup>, *Myd88*<sup>-/-</sup>, or *Trif*<sup>+/+</sup> mice. Cells were treated with α-GalCer (100 ng/ml), PI57 (2.5, 5, or 10 μg/ml), PBS30 (1, 2.5, or 5 μg/ml), or vehicle for 48 hours. IFN-γ and IL-4 were measured by ELISA. (C) IL-2 production from hybridomas derived from invariant Vα14 NKT cells (RT2, RT23, and RT24) and an irrelevant Vβ8<sup>+</sup> T cell (RT8; control) (see Supplemental Methods). (D) Mouse NKT cell lines were stained with PE-labeled CD1d tetramers of PI57 or α-GalCer at 4°C for 45 minutes or 37°C for 25 minutes, and with anti-TCRβ-APC antibody. Top: Lymphocytes were gated in the FSC/SSC window. Bottom: Percentage of CD1d tetramer<sup>+</sup> cells. (E) IFN-γ and IL-4 production from human NKT cell lines by treatment with α-GalCer (100 ng/ml), PI57 (10 μg/ml), or vehicle for 48 hours in vitro (see Supplemental Methods). (F) IFN-γ production from CD1d-transfected NKT cell clone BM2a.3 in presence of PI57 and blocking mAb against human CD1d or CD1b (see Supplemental Methods). (G) CD1d Fc-coated Maxisorp plates were loaded with lipid and cultured with 5 × 10<sup>4</sup> NKT cells. IFN-γ was analyzed by ELISA after 24 hours. Data represent 3 or 5 independent experiments.

subpopulation of NKT cells that can suppress the effects of other subpopulations of NKT cells that enhance the development of experimental asthma. These results suggest that a balance exists between NKT cells that induce, and those that protect against, AHR, and that stimulation with H3N1, α-C-GalCer, or *H. pylori* glycolipids, but not a *Sphingomonas* glycolipid or α-GalCer, may selectively expand this regulatory NKT cell population in young mice. The inability of

α-GalCer to protect may be due to the fact that it nonselectively stimulates all invariant NKT cells or because it may anergize NKT cells, including suppressive populations. Nevertheless, these data support the idea that under normal, pathogen-free conditions, CD4<sup>+</sup> NKT cells that induce AHR predominate, but that in very young mice, exposure to Th1-skewing reagents that can alter the composition of NKT cell subpopulations may change subsequent lung immunity.



Therefore, it appears that the balance between CD4<sup>+</sup> versus regulatory (presumably DN) NKT cells is determined or imprinted early in life but might be influenced by exposure to specific types of infections, particularly those that can affect NKT cells. In our studies, H3N1 infection in 2-week-old pups activated the immature NKT cells and preferentially expanded a DN NKT cell subset. In addition, our studies suggest that  $\alpha$ -C-GalCer and glycolipids from *H. pylori* can profoundly affect this NKT cell subpopulation, which may explain epidemiological studies showing an association of *H. pylori* infection with protection against asthma (2, 3). Although these studies were performed in mice, which mature from neonates to adults in only 35 days versus many years in humans, taken together, our results suggest that infection with certain microorganisms can prevent the subsequent development of asthma and allergy by expanding the relative proportion of a specific subset of NKT cells, thus providing an immunological mechanism for the hygiene hypothesis. Finally, these results predict that treatment of children with compounds such as  $\alpha$ -C-GalCer and others derived from microorganisms (e.g., *H. pylori*) might expand this regulatory NKT cell subset and be effective in preventing the development of asthma.

## Methods

**Mice.** WT BALB/c ByJ and *Tbet*<sup>-/-</sup> (C.129S6-Tbx21tm1Glm/J) mice were purchased from The Jackson Laboratory. *Ja.18*<sup>-/-</sup> mice were gifts from M. Taniguchi and T. Nakayama (Chiba University, Chiba, Japan). *Tlr7*<sup>-/-</sup> mice were generated by Shizuo Akira, and the *V $\alpha$ 14* Tg mice were provided by Albert Bendelac (University of Chicago, Chicago, Illinois, USA). These strains were backcrossed to BALB/c for more than 10 generations. DO11.10 X *Rag*<sup>-/-</sup> mice were provided by Abul Abbas (UCSF, San Francisco, California, USA). For studies in suckling mice, BALB/c, *Tlr7*<sup>-/-</sup>, and *Tbet*<sup>-/-</sup> mice were bred, and the offspring were infected at 2 weeks of age, then weaned at 3 weeks. The Animal Care and Use Committee at Children's Hospital Boston approved all animal protocols.

**Influenza A infection.** Two-week-old pups (suckling mice) or 8-week-old adult mice were anesthetized with 3% isoflurane and inoculated intranasally (i.n.) with influenza A virus (strain Mem/71 [H3N1]) in 20  $\mu$ l PBS for suckling mice or 50  $\mu$ l PBS for adult mice. The virus is a reassortant influenza virus strain carrying the hemagglutinin of A/Memphis/1/71 (H3) and the neuraminidase of A/Bellamy/42 (N1). The virus was grown and harvested from 10-day embryonated chicken eggs as previously described (59). The dose of virus used ( $1.2 \times 10^4$  PFU/mouse) causes nonlethal pneumonia of both suckling and adult mice, with complete virus clearance around day 7 after infection. Control (mock-infected) mice were treated with i.n. allantoic fluid (AF) diluted 1:500 in PBS.

**Reagents.**  $\alpha$ -GalCer and PBS30 (31) were synthesized by P.B. Savage (Brigham Young University, Provo, Utah, USA). *H. pylori* glycolipids were extracted and purified as described in the Supplemental Methods. The *H. pylori* glycolipid PI57 (cholesteryl 6-O-tetradecanoyl- $\alpha$ -D-glucopyranoside) was synthesized based on <sup>1</sup>H, <sup>13</sup>C NMR spectrometry, TLC analysis, ES-mass spectrometry of lipids from *H. pylori* SS1 and human *H. pylori* S strains (Supplemental Figure 4 and Supplemental Methods), and data reported for purified *H. pylori* glycolipids (30). An analog of  $\alpha$ -C-GalCer, called "GCK151", which has activity with mouse and human NKT cells (27), was synthesized by Richard W. Franck (Hunter College of CUNY).

**PI57-loaded CD1d tetramers.** To generate PI57-loaded mCD1d monomers, a 10-fold molar excess of PI57 in DMSO at 2 mg/ml was incubated with biotinylated-mCD1d (from the NIH Tetramer facility) in 2 mM CHAPS and 20 mM Tris pH 7.0 overnight at room temperature. The mCD1d monomers were tetramerized by adding SA-PE (S868; Invitrogen) to the lipid-loaded monomers as previously described (60).

**Induction of AHR and measurement of airway responsiveness in the OVA model.** To induce AHR, BALB/c mice were sensitized with 100  $\mu$ g of OVA (Sigma-Aldrich) in alum administered i.p. (on day 0). After sensitization, mice were exposed to i.n. antigen (50  $\mu$ g OVA/day) or normal saline for 1 day (day 7; single-dose challenge protocol) or for 3 consecutive days (days 7–9). AHR was assessed on the day after last OVA challenge. Control mice received i.p. injection of PBS and i.n. administrations of normal saline.

**Collection and analysis of bronchoalveolar lavage.** Immediately after the AHR measurement, mice were euthanized and the lungs were lavaged twice with 0.5 ml of PBS, and the fluid was pooled. Cells in bronchoalveolar lavage (BAL) were counted and analyzed as previously described (20). The relative number of different types of leukocytes was determined from slide preparations of BAL stained with Diff-Quik solution (Dade Behring).

**Adoptive transfer of NKT cells.** NKT cells were purified from splenocytes of WT BALB/c, influenza virus-infected BALB/c, influenza virus-infected *Tlr7*<sup>-/-</sup>, influenza virus-infected *Tbet*<sup>-/-</sup>, *V $\alpha$ 14* TCR transgenic mice, PI57-treated BALB/c, and  $\alpha$ -GalCer-treated BALB/c mice using magnetic cell sorting (MACS), as previously described (20). Splenic NKT cells were labeled with PE-conjugated CD1d tetramer, followed by anti-PE microbeads (Miltenyi Biotec) and then sorted with AutoMACS according to the manufacturer's instruction. Purity of NKT cells was approximately 93% (Supplemental Figure 2A), and there was no detectable Treg cell contamination (Supplemental Figure 2B). Purified NKT cells were adoptively transferred into immunized recipient mice by intravenous injection ( $10^6$  for *Ja.18*<sup>-/-</sup>;  $5 \times 10^5$  for BALB/c) 1 hour before the first challenge of OVA (day 7). For the OVA-specific Treg cell experiment,  $5 \times 10^4$  DO11.10 CD4<sup>+</sup> T cells (from DO11.10 X *Rag*<sup>-/-</sup> mice) were adoptively transferred into recipient mice 5 hours before sensitization with OVA/alum (day 0). The recipients later received NKT cells 1 hour before the first challenge of OVA (day 7).

**ELISA.** Mouse or human IL-4 and IFN- $\gamma$  levels were measured by ELISA, as previously described (20). Mean values of triplicate cultures were shown. Data are representative of 2 or 3 independent experiments.

**Statistics.** Differences between groups with parametric distributions were analyzed using the Student's 2-tailed *t* test. Otherwise, the Mann-Whitney *U* test was used. Data represent mean  $\pm$  SEM. *P* values of 0.05 or less were considered statistically significant.

## Acknowledgments

These studies were supported by grants from the NIH RO1 AI68085, RO1 HL62348, RO1 AI026322, and RC1 HL069507, by an award from the Bunning Food Allergy Project, and by grant 20570146 from the Ministry of Education, Culture, Sports, Science, and Technology of Japan. The authors thank Dirk Zajonc for help in loading CD1d molecules, and the NIH NIAID Tetramer Facility for providing CD1d monomers and PBS57-CD1d tetramers.

Received for publication August 20, 2010, and accepted in revised form October 20, 2010.

Address correspondence to: Dale T. Umetsu, Karp Labs, Rm 10127, One Blackfan Circle, Boston, Massachusetts 02115, USA. Phone: 617.919.2439; Fax: 617.730.0384; E-mail: dale.umetsu@childrens.harvard.edu. Or to: Michio Shimamura, Tsukuba Research Center for Interdisciplinary Materials Science, University of Tsukuba, 1-1-1 Tennodai, Ibaraki 305-8571, Japan. Phone: 81.29.853.4527; Fax: 81.29.853.4507; E-mail: michio@chem.tsukuba.ac.jp. Or to: Petr Illarionov, University of Birmingham School of Biosciences, Edgbaston B15 2TT, Birmingham, United Kingdom. Phone: 44.121.4158123; Fax: 44.121.4145925; E-mail: illar@yahoo.com.





1. Strachan DP. Hay fever, hygiene, and household size. *BMJ*. 1989;299(6710):1259–1260.
2. Matricardi P, et al. Exposure to foodborne and orofecal microbes versus airborne viruses in relation to atopy and allergic asthma: epidemiological study. *BMJ*. 2000;320(7232):412–417.
3. Reibman J, et al. Asthma is inversely associated with *Helicobacter pylori* status in an urban population. *PLoS One*. 2008;3(12):e4060.
4. Braun-Fahrlander C, et al. Environmental exposure to endotoxin and its relation to asthma in school-age children. *N Engl J Med*. 2002;347(12):869–877.
5. Conrad ML, et al. Maternal TLR signaling is required for prenatal asthma protection by the nonpathogenic microbe *Acinetobacter lwoffii* F78. *J Exp Med*. 2009;206(13):2869–2877.
6. Matricardi PM, et al. Cross sectional retrospective study of prevalence of atopy among Italian military students with antibodies against hepatitis A virus. *BMJ*. 1997;314(7086):999–1003.
7. Matricardi PM, Rosmini F, Panetta V, Ferrigno L, Bonini S. Hay fever and asthma in relation to markers of infection in the United States. *J Allergy Clin Immunol*. 2002;110(3):381–387.
8. Jackson DJ, et al. Wheezing rhinovirus illnesses in early life predict asthma development in high-risk children. *Am J Respir Crit Care Med*. 2008;178(7):667–672.
9. Martinez FD, et al. Asthma and wheezing in the first six years of life. *New Engl J Med*. 1995;332(3):133–138.
10. von Mutius E, Martinez FD, Fritzsche C, Nicolai T, Roell G, Thiemann HH. Prevalence of asthma and atopy in two areas of West and East Germany. *Am J Respir Crit Care Med*. 1994;149(2 pt 1):358–364.
11. Tsitoura DC, Kim S, Dabbagh K, Berry G, Lewis DB, Umetsu DT. Respiratory infection with influenza A virus interferes with the induction of tolerance to aeroallergens. *J Immunol*. 2000;165(6):3484–3491.
12. Dahl M, Dabbagh K, Liggitt D, Kim S, Lewis D. Viral-induced T helper type 1 responses enhance allergic disease by effects on lung dendritic cells. *Nat Immunol*. 2004;5(3):337–343.
13. Marsland B, Harris N, Camberis M, Kopf M, Hook S, Le Gros G. Bystander suppression of allergic airway inflammation by lung resident memory CD8+ T cells. *Proc Natl Acad Sci U S A*. 2004;101(16):6116–6121.
14. Wohlleben G, et al. Influenza A virus infection inhibits the efficient recruitment of Th2 cells into the airways and the development of airway eosinophilia. *J Immunol*. 2003;170(9):4601–4611.
15. Glezen WP, Greenberg SB, Atmar RL, Piedra PA, Couch RB. Impact of respiratory virus infections on persons with chronic underlying conditions. *JAMA*. 2000;283(4):499–505.
16. Miller EK, et al. Influenza burden for children with asthma. *Pediatrics*. 2008;121(1):1–8.
17. Jain S, et al. Hospitalized patients with 2009 H1N1 influenza in the United States, April–June 2009. *N Engl J Med*. 2009;361(20):1935–1944.
18. De Santo C, et al. Invariant NKT cells reduce the immunosuppressive activity of influenza A virus-induced myeloid-derived suppressor cells in mice and humans. *J Clin Invest*. 2008;118(12):4036–4048.
19. Matangkasombut P, Pichavant M, Dekruyff RH, Umetsu DT. Natural killer T cells and the regulation of asthma. *Mucosal Immunol*. 2009;2(5):383–392.
20. Akbari O, et al. Essential role of NKT cells producing IL-4 and IL-13 in the development of allergen-induced airway hyperreactivity. *Nature Medicine*. 2003;9(5):582–588.
21. Pichavant M, et al. Ozone exposure in a mouse model induces airway hyperreactivity that requires the presence of natural killer T cells and IL-17. *J Exp Med*. 2008;205(2):385–393.
22. Kim EY, et al. Persistent activation of an innate immune response translates respiratory viral infection into chronic lung disease. *Nat Med*. 2008;14(6):633–640.
23. Townsend MJ, et al. T-bet regulates the terminal maturation and homeostasis of NK and Valpha14i NKT cells. *Immunity*. 2004;20(4):477–494.
24. Kim HY, et al. The development of airway hyperreactivity in T-bet-deficient mice requires CD1d-restricted NKT cells. *J Immunol*. 2009;182(5):3252–3261.
25. Schmiege J, Yang G, Franck RW, Tsuji M. Superior protection against malaria and melanoma metastases by a C-glycoside analogue of the natural killer T cell ligand alpha-Galactosylceramide. *J Exp Med*. 2003;198(11):1631–1641.
26. Fujii S, et al. Glycolipid alpha-C-galactosylceramide is a distinct inducer of dendritic cell function during innate and adaptive immune responses of mice. *Proc Natl Acad Sci U S A*. 2006;103(30):11252–11257.
27. Li X, Chen G, Garcia-Navarro R, Franck RW, Tsuji M. Identification of C-glycoside analogues that display a potent biological activity against murine and human invariant natural killer T cells. *Immunology*. 2009;127(2):216–225.
28. Wunder C, et al. Cholesterol glucosylation promotes immune evasion by *Helicobacter pylori*. *Nat Med*. 2006;12(9):1030–1038.
29. Linz B, et al. An African origin for the intimate association between humans and *Helicobacter pylori*. *Nature*. 2007;445(7130):915–918.
30. Hirai Y, Haque M, Yoshida T, Yokota K, Yasuda T, Oguma K. Unique cholesteryl glucosides in *Helicobacter pylori*: composition and structural analysis. *J Bacteriol*. 1995;177(18):5327–5333.
31. Mattner J, et al. Exogenous and endogenous glycolipid antigens activate NKT cells during microbial infections. *Nature*. 2005;434(7032):525–529.
32. Kinjo Y, et al. Recognition of bacterial glycosphingolipids by natural killer T cells. *Nature*. 2005;434(7032):520–525.
33. Bendelac A, Savage PB, Teyton L. The biology of NKT cells. *Annu Rev Immunol*. 2007;25:297–336.
34. Savage AK, et al. The transcription factor PLZF directs the effector program of the NKT cell lineage. *Immunity*. 2008;29(3):391–403.
35. Kreslavsky T, et al. TCR-inducible PLZF transcription factor required for innate phenotype of a subset of gamma delta T cells with restricted TCR diversity. *Proc Natl Acad Sci U S A*. 2009;106(30):12453–12458.
36. Kadowaki N, et al. Distinct cytokine profiles of neonatal natural killer T cells after expansion with subsets of dendritic cells. *J Exp Med*. 2001;193(10):1221–1226.
37. D'Andrea A, et al. Neonatal invariant Valpha24+ NKT lymphocytes are activated memory cells. *Eur J Immunol*. 2000;30(6):1544–1550.
38. Kronenberg M. Toward an understanding of NKT cell biology: progress and paradoxes. *Annu Rev Immunol*. 2005;23:877–900.
39. Kinjo Y, et al. Natural killer T cells recognize diacylglycerol antigens from pathogenic bacteria. *Nat Immunol*. 2006;7(9):978–986.
40. Mattner J, et al. Exogenous and endogenous glycolipid antigens activate NKT cells during microbial infections. *Nature*. 2005;434(7032):525–529.
41. Brigl M, Bry L, Kent SC, Gumperz JE, Brenner MB. Mechanism of CD1d-restricted natural killer T cell activation during microbial infection. *Nat Immunol*. 2003;4(12):1230–1237.
42. Kim S, Lalani S, Parekh VV, Vincent TL, Wu L, Van Kaer L. Impact of bacteria on the phenotype, functions, and therapeutic activities of invariant NKT cells in mice. *J Clin Invest*. 2008;118(6):2301–2315.
43. Fischer K, et al. Mycobacterial phosphatidylinositol mannoside is a natural antigen for CD1d-restricted T cells. *Proc Natl Acad Sci U S A*. 2004;101(29):10685–10690.
44. Sada-Ovalle I, Chiba A, Gonzales A, Brenner MB, Behar SM. Innate invariant NKT cells recognize *Mycobacterium tuberculosis*-infected macrophages, produce interferon-gamma, and kill intracellular bacteria. *PLoS Pathog*. 2008;4(12):e1000239.
45. Arnold I, et al. Tolerance rather than immunity protects from *Helicobacter pylori*-induced gastric preneoplasia [published online ahead of print June 23, 2010]. *Gastroenterology*. doi:10.1053/j.gastro.2010.06.047.
46. Lebrun AH, et al. Cloning of a cholesterol-alpha-galactosyltransferase from *Helicobacter pylori*. *J Biol Chem*. 2006;281(38):27765–27772.
47. Lisbonne M, et al. Cutting edge: invariant V alpha 14 NKT cells are required for allergen-induced airway inflammation and hyperreactivity in an experimental asthma model. *J Immunol*. 2003;171(4):1637–1641.
48. Akbari O, et al. CD4+ invariant T-cell-receptor+ natural killer T cells in bronchial asthma. *N Engl J Med*. 2006;354(11):1117–1129.
49. Vijayanand P, et al. Invariant natural killer T cells in asthma and chronic obstructive pulmonary disease. *N Engl J Med*. 2007;356(14):1410–1422.
50. Stock P, Lombardi V, Kohlrantz V, Akbari O. Induction of airway hyperreactivity by IL-25 is dependent on a subset of invariant NKT cells expressing IL-17RB. *J Immunol*. 2009;182(8):5116–5122.
51. Terashima A, et al. A novel subset of mouse NKT cells bearing the IL-17 receptor B responds to IL-25 and contributes to airway hyperreactivity. *J Exp Med*. 2008;205(12):2727–2733.
52. Hachem P, et al. Alpha-galactosylceramide-induced iNKT cells suppress experimental allergic asthma in sensitized mice: role of IFN-gamma. *Eur J Immunol*. 2005;35(10):2793–2802.
53. Wilson SB, et al. Extreme Th1 bias of invariant Valpha24/alphaQ T cells in type 1 diabetes. *Nature*. 1998;391(6663):177–181.
54. Diana J, et al. NKT cell-plasmacytoid dendritic cell cooperation via OX40 controls viral infection in a tissue-specific manner. *Immunity*. 2009;30(2):289–299.
55. Seino KI, et al. Requirement for natural killer T (NKT) cells in the induction of allograft tolerance. *Proc Natl Acad Sci U S A*. 2001;98(5):2577–2581.
56. Zeng D, et al. Bone marrow NK1.1(-) and NK1.1(+) T cells reciprocally regulate acute graft versus host disease. *J Exp Med*. 1999;189(7):1073–1081.
57. Lowsky R, et al. Protective conditioning for acute graft-versus-host disease. *N Engl J Med*. 2005;353(13):1321–1331.
58. Pillai AB, George TI, Dutt S, Strober S. Host natural killer T cells induce an interleukin-4-dependent expansion of donor CD4+CD25+Foxp3+ T regulatory cells that protects against graft-versus-host disease. *Blood*. 2009;113(18):4458–4467.
59. Baumgarth N, Brown L, Jackson D, Kelso A. Novel features of the respiratory tract T-cell response to influenza virus infection: lung T cells increase expression of gamma interferon mRNA in vivo and maintain high levels of mRNA expression for interleukin-5 (IL-5) and IL-10. *J Virol*. 1994;68(11):7575–7581.
60. Liu Y, et al. A modified alpha-galactosyl ceramide for staining and stimulating natural killer T cells. *J Immunol Methods*. 2006;312(1–2):34–39.

## REVIEW ARTICLE

**Bioinformatics approach to identifying molecular biomarkers and networks in multiple sclerosis**

Jun-ichi Satoh

Department of Bioinformatics and Molecular Neuropathology, Meiji Pharmaceutical University, Tokyo, Japan

**Keywords**

bioinformatics; KeyMolnet; molecular network; multiple sclerosis; systems biology

**Correspondence**

Jun-ichi Satoh MD, PhD, Department of Bioinformatics and Molecular Neuropathology, Meiji Pharmaceutical University, 2-522-1 Noshio, Kiyose, Tokyo 204-8588, Japan.

Tel: +81-42-495-8678

Fax: +81-42-495-8678

Email: satoj@my-pharm.ac.jp

Received: 6 June 2010; accepted: 3 August 2010.

**Abstract**

Multiple sclerosis (MS) is an inflammatory demyelinating disease of the central nervous system (CNS) white matter mediated by an autoimmune process triggered by a complex interplay between genetic and environmental factors, in which the precise molecular pathogenesis remains to be comprehensively characterized. The global analysis of genome, transcriptome, proteome and metabolome, collectively termed omics, promotes us to characterize the genome-wide molecular basis of MS. However, as omics studies produce high-throughput experimental data at one time, it is often difficult to find out the meaningful biological implications from huge datasets. Recent advances in bioinformatics and systems biology have made major breakthroughs by illustrating the cell-wide map of complex molecular interactions with the aid of the literature-based knowledgebase of molecular pathways. The integration of omics data derived from the disease-affected cells and tissues with underlying molecular networks provides a rational approach not only to identifying the disease-relevant molecular markers and pathways, but also to designing the network-based effective drugs for MS. (Clin. Exp. Neuroimmunol. doi: 10.1111/j.1759-1961.2010.00013.x, September 2010)

**Introduction**

Multiple sclerosis (MS) is an inflammatory demyelinating disease affecting exclusively the central nervous system (CNS) white matter mediated by an autoimmune process triggered by a complex interplay between genetic and environmental factors.<sup>1</sup> Intravenous administration of interferon-gamma (IFN $\gamma$ ) provoked acute relapses of MS, indicating a pivotal role of proinflammatory T helper type 1 (Th1) lymphocytes. More recent studies proposed the pathogenic role of Th17 lymphocytes in sustained tissue damage in MS.<sup>2</sup> MS shows a great range of phenotypic variability. The disease is classified into relapsing-remitting MS (RRMS), secondary progressive MS (SPMS) or primary progressive MS (PPMS) with respect to the clinical course. Pathologically, MS shows a remarkable heterogeneity in the degree of inflammation, complement activation, antibody deposition, demyelination and

remyelination, oligodendrocyte apoptosis, and axonal degeneration.<sup>3</sup> Currently available drugs in clinical practice of MS, including interferon-beta (IFN $\beta$ ), glatiramer acetate, mitoxantrone, FTY720 and natalizumab, have proven only limited efficacies in subpopulations of the patients.<sup>4</sup> These observations suggest the hypothesis that MS is a kind of neurological syndrome caused by different immunopathological mechanisms leading to the final common pathway that provokes inflammatory demyelination. Therefore, the identification of specific biomarkers relevant to the heterogeneity of MS is highly important to establish the molecular mechanism-based personalized therapy in MS.

After the completion of the Human Genome Project in 2003, the global analysis of genome, transcriptome, proteome and metabolome, collectively termed omics, promotes us to characterize the genome-wide molecular basis of the diseases, and helps us to identify disease-specific molecular signatures

and biomarkers for diagnosis and prediction of prognosis. Actually, the genome-wide association study (GWAS) of MS revealed novel risk alleles for susceptibility of MS.<sup>5</sup> The comprehensive transcriptome and proteome profiling of brain tissues and lymphocytes identified key molecules aberrantly regulated in MS, whose role has not been previously predicted in the pathogenesis of MS.<sup>6,7</sup> Most recently, the application of next-generation sequencing technology to personal genomes has enabled us to investigate the genetic basis of MS at the level of individual patients.<sup>8</sup>

Because omics studies usually produce high-throughput experimental data at one time, it is often difficult to find out the meaningful biological implications from such a huge dataset. Recent advances in bioinformatics and systems biology have made major breakthroughs by showing the cell-wide map of complex molecular interactions with the aid of the literature-based knowledgebase of molecular pathways.<sup>9</sup> The logically arranged molecular networks construct the whole system characterized by robustness, which maintains the proper function of the system in the face of genetic and environmental perturbations.<sup>10</sup> In the scale-free molecular network, targeted disruption of limited numbers of critical components designated the hub, on which the biologically important molecular connections concentrate, could disturb the whole cellular function by destabilizing the network.<sup>11</sup> From the point of these views, the integration of omics data derived from the disease-affected cells and tissues with underlying molecular networks provides a rational approach not only to characterizing the disease-relevant pathways, but also to identifying the network-based effective drug targets.

Increasing numbers of human disease-oriented omics data have been deposited in public databases, such as the Gene Expression Omnibus (GEO) repository (<http://www.ncbi.nlm.nih.gov/geo>) and the ArrayExpress archive (<http://www.ebi.ac.uk/microarray-as/ae>). Most of these are transcriptome datasets. Importantly, they really include the data that have potentially valuable information on molecular biomarkers and networks of the diseases, when they are reanalyzed by appropriate bioinformatics approaches, followed by validation of *in silico* observations with *in vitro* and *in vivo* experiments.<sup>12</sup>

The present review has focused on bioinformatics approaches to identifying MS-associated molecular biomarkers and networks from high-throughput data of omics studies.

### Global gene expression analysis

DNA microarray technology is an innovative approach that allows us to systematically monitor the genome-wide gene expression pattern of disease-affected tissues and cells. This approach enables us to illustrate most efficiently a global picture of cellular activity by the messenger RNA (mRNA) expression levels as an indicator, although the levels of mRNA do not always correlate with the levels of proteins directly involved in cellular function. However, the use of DNA microarray is more convenient to collect temporal and spatial snapshots of gene expression than the conventional mass spectrometry, which is often hampered by limited resolution of protein separation. In transcriptome analysis, we could logically assume that a set of coregulated genes might have similar biological functions within the cells.

First of all, I would like to briefly overview the gene expression analysis (Fig. 1). In general, total RNA fractions containing mRNA species are extracted from cells and tissues, individually labeled with fluorescent dyes, and processed for hybridization with thousands of oligonucleotides of known sequences immobilized on the arrays. After washing, they are processed for signal acquisition on a scanner. Various types of microarrays are currently available, although the MicroArray Quality Control (MAQC) project verified that the core results are well reproducible among different platforms used.<sup>13</sup> However, it is recommended that each experiment should contain biological replicates to validate reproducibility of the observations. The raw data are normalized by representative methods, including the quantile normalization method and the Robust MultiChip Average (RMA) method using the R software of the Bioconductor package ([cran.r-project.org](http://cran.r-project.org)) or the GENESPRING software (Agilent Technology, Palo Alto, CA, USA).

To identify differentially expressed genes (DEG) among distinct samples, the normalized data are processed for statistical analysis using *t*-test for comparison between two groups or analysis of variance (ANOVA) for comparison among more than three groups, followed by the multiple comparison test with the Bonferroni correction or by controlling false discovery rate (FDR) below 0.05 to adjust *P*-values.

In the next step, the levels of expression of DEG should be validated by quantitative reverse transcription polymerase chain reaction (qRT-PCR). The normalized data are also processed for hierarchical

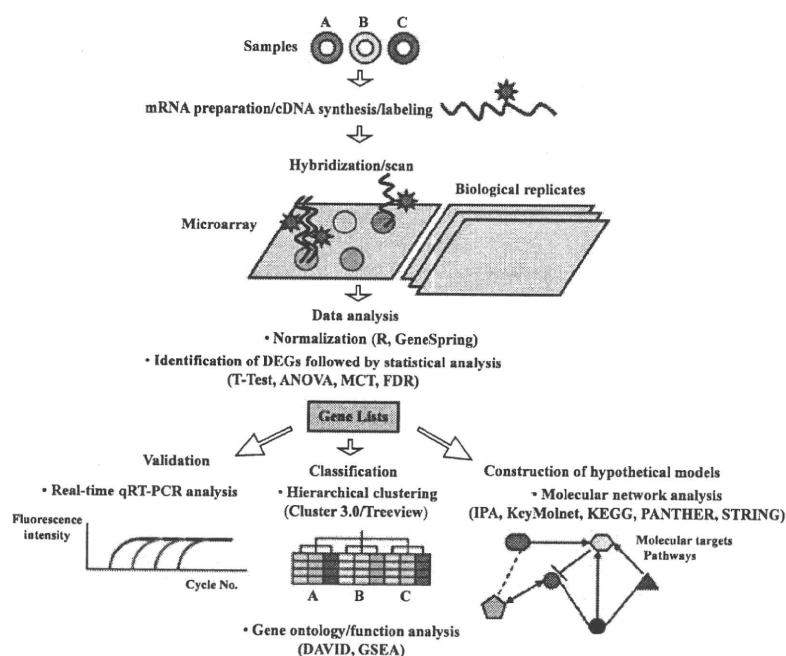


**Figure 1** The load map from global gene expression profiling to molecular network analysis. Total RNA samples labeled with fluorescent dyes are processed for hybridization with oligonucleotide probes on the arrays, which should include biological replicates. They are processed for signal acquisition on a scanner. To identify the list of differentially expressed genes (DEG) among the samples, the normalized data are processed for statistical analysis, followed by validation by quantitative reverse transcription polymerase chain reaction (qRT-PCR). They are also processed for hierarchical clustering analysis and gene ontology and function analysis. To identify biologically relevant molecular pathways, the list of DEG is imported into pathway analysis tools endowed with a comprehensive knowledgebase. ANOVA, analysis of variance; DAVID, Database for Annotation, Visualization and Integrated Discovery; FDR, false discovery rate; GSEA, Gene Set Enrichment Analysis; IPA, Ingenuity Pathways Analysis; KEGG, Kyoto Encyclopedia of Genes and Genomes; MCT, multiple comparison test; PANTHER, Protein Analysis Through Evolutionary Relationships; and STRING; Search Tool for the Retrieval of Interacting Genes/Proteins.

clustering analysis to classify the expression of profile-based groups of genes and samples by using GENESPRING or the open-access resources, such as CLUSTER 3.0 ([bonsai.ims.u-tokyo.ac.jp/~mdphoon/software/cluster](http://bonsai.ims.u-tokyo.ac.jp/~mdphoon/software/cluster)) and TREEVIEW ([sourceforge.net/projects/jtreeview](http://sourceforge.net/projects/jtreeview)). The Gene ID Conversion tool of the Database for Annotation, Visualization and Integrated Discovery (DAVID) ([david.abcc.ncifcrf.gov](http://david.abcc.ncifcrf.gov))<sup>14</sup> converts the large-scale array-specific probe IDs into the corresponding Entrez Gene IDs, HUGO Gene Symbols, Ensembl Gene IDs or UniProt IDs, being more convenient for application to the downstream analysis. Both the DAVID Functional annotation tool and the Gene Set Enrichment Analysis (GSEA) tool ([www.broad.mit.edu/gsea/downloads.jsp](http://www.broad.mit.edu/gsea/downloads.jsp))<sup>15</sup> are open-access resources that help us to identify a set of enriched genes with a specified functional annotation in the entire list of genes. Many other approaches for preprocessing microarray data are applicable, and the resources are available elsewhere.

### Molecular network analysis

To identify biologically relevant molecular pathways from large-scale data, we could analyze them by using a battery of pathway analysis tools endowed with a comprehensive knowledgebase; that is, Kyoto Encyclopedia of Genes and Genomes (KEGG; <http://www.kegg.jp>), the Protein Analysis Through Evolutionary Relationships (PANTHER) classification system (<http://www.pantherdb.org>), Search Tool for the Retrieval of Interacting Genes/Proteins (STRING; [string.embl.de](http://string.embl.de)), Ingenuity Pathways Analysis (IPA; Ingenuity Systems, <http://www.ingenuity.com>) and KeyMolnet (Institute of Medicinal Molecular Design, <http://www.immd.co.jp>) (Fig. 1). KEGG, PANTHER and STRING are open-access databases, whereas IPA and KeyMolnet are commercial databases updated regularly. Both transcriptome and proteome data are acceptable for all the databases described here.

KEGG systematically integrates genomic and chemical information to create the whole biological



system *in silico*.<sup>16</sup> KEGG includes manually curated reference pathways that cover a wide range of metabolic, genetic, environmental and cellular processes, and human diseases. Currently, KEGG contains 108 983 pathways generated from 358 reference pathways. PANTHER, operating on the computational algorithms that relate the evolution of protein sequences to the evolution of protein functions and biological roles, provides a structured representation of protein function in the context of biological reaction networks.<sup>17</sup> PANTHER includes the information on 165 regulatory and metabolic pathways, manually curated by expert biologists. By uploading the list of Gene IDs, the PANTHER gene expression data analysis tool identifies the genes in terms of over- or under-representation in canonical pathways, followed by statistical evaluation by multiple comparison test with the Bonferroni correction. STRING is a database that contains physiological and functional protein-protein interactions composed of 2 590 259 proteins from 630 organisms.<sup>18</sup> STRING integrates the information from numerous sources, including experimental repositories, computational prediction methods and public text collections. By uploading the list of UniProt IDs, STRING illustrates the union of all possible association networks.

IPA is a knowledgebase that contains approximately 2 270 000 biological and chemical interactions and functional annotations with definite scientific evidence, curated by expert biologists.<sup>19</sup> By uploading the list of Gene IDs and expression values, the network-generation algorithm identifies focused genes integrated in a global molecular network. IPA calculates the score  $P$ -value, the statistical significance of association between the genes and the networks by the Fisher's exact test.

KeyMolnet contains knowledge-based content on 123 000 relationships among human genes and proteins, small molecules, diseases, pathways and drugs, curated by expert biologists.<sup>20</sup> They are categorized into the core content collected from selected review articles with the highest reliability or the secondary contents extracted from abstracts of PubMed and Human Reference Protein database (HPRD). By importing the list of Gene ID and expression values, KeyMolnet automatically provides corresponding molecules as a node on networks. The "common upstream" network-search algorithm enables us to extract the most relevant molecular network composed of the genes coordinately regulated by putative common upstream transcription factors. The "neighboring" network-search algorithm selected one or more molecules as starting points to generate

the network of all kinds of molecular interactions around starting molecules, including direct activation/inactivation, transcriptional activation/repression, and the complex formation within the designated number of paths from starting points. The "N-points to N-points" network-search algorithm identifies the molecular network constructed by the shortest route connecting the start-point molecules and the end-point molecules. The generated network was compared side-by-side with 430 human canonical pathways of the KeyMolnet library. The algorithm counting the number of overlapping molecular relations between the extracted network and the canonical pathway makes it possible to identify the canonical pathway showing the most significant contribution to the extracted network. The significance in the similarity between both is scored following the formula, where  $O$  is the number of overlapping molecular relations between the extracted network and the canonical pathway,  $V$  is the number of molecular relations located in the extracted network,  $C$  is the number of molecular relations located in the canonical pathway,  $T$  is the number of total molecular relations, and  $X$  is the sigma variable that defines coincidence.

$$\text{Score} = -\log_2(\text{Score}[P])$$

$$\text{Score}(P) = \sum_{x=O}^{\text{Min}(C,V)} f(x)$$

$$f(x) = c C_x \cdot T - C C_{V-x} / T C_V$$

### Biomarkers for predicting MS relapse

Molecular mechanisms underlying acute relapse of MS remain currently unknown. If molecular biomarkers for MS relapse are identified, we could predict the timing of relapses, being invaluable to start the earliest preventive intervention.

By gene expression profiling with Affymetrix Human Genome U133 plus 2.0 arrays, Corvol et al. identified 975 genes that separate clinically isolated syndrome (CIS) into four groups.<sup>21</sup> Surprisingly, 92% of patients in group 1 were characterized by a subset of 108 genes converted to clinically definite MS (CDMS) within 9 months of the first attack. They suggest downregulation of TOB1, a negative regulator of T cell proliferation as a marker predicting the conversion from CIS to CDMS.

By gene expression profiling with Affymetrix Human Genome U133A2 arrays, Achiron et al. showed that 1578 DEG of peripheral blood mononuclear cells (PBMC) of RRMS patients, differentiating

acute relapse from remission, are enriched in the apoptosis-related pathway, in which proapoptotic genes are downregulated, whereas antiapoptotic genes are upregulated during acute relapse.<sup>22</sup> The same group also compared 62 patients with CDMS and 32 patients with CIS by combining gene expression profiling with the support vector machine (SVM)-based prediction of time to the next acute relapse, setting a two stage predictor composed of First Level Predictors (FLP) and Fine Turning Predictors (FTP).<sup>23</sup> They identified three sets of the best 10-gene FLP that predict the next relapse with a resolution of 500 days and four sets of the best 9-gene FTP that predict the forthcoming relapse with a resolution of 50 days. The predictor genes are enriched in the TGF $\beta$ 2-related signaling pathway. More recently, Achiron et al. compared nine subjects who developed MS during a 9-year follow-up period (the preactive stage of MS; MS-to-be) and 11 control subjects unaffected with MS (MS-free) by gene expression profiling.<sup>24</sup> They found downregulation of nuclear receptor NR4A1 in the preactive stage of MS, suggesting that self-reactive T cells are not eliminated in the MS-to-be population, owing to a defect in the NR4A1-dependent apoptotic mechanism.

By gene expression profiling with a custom microarray of the Peter MacCallum Cancer Institute, Arthur et al. showed that a set of dysregulated genes in peripheral blood cells during the relapse and the remission phases of RRMS are enriched in the categories involved in apoptosis and inflammation, when annotated according to the GOstat program.<sup>25</sup> They also found upregulation of TGF $\beta$ 1 during the relapse. These observations support the working hypothesis that MS relapse involves an imbalance between promoting and preventing apoptosis of autoreactive and regulatory T cells. By gene expression analysis with Affymetrix Human Genome U133 plus 2.0 arrays, Brynedal et al. showed that MS relapses reflect the gene expression change in PBMC, but not in cerebrospinal fluid (CSF) lymphocytes, suggesting the importance of initial events triggering relapses occurring outside the CNS.<sup>26</sup>

By gene expression profiling with a custom DNA microarray (Hitachi Life Science, Saitama, Japan), we identified 43 DEG in peripheral blood CD3<sup>+</sup> T cells between the peak of acute relapse and the complete remission of RRMS patients.<sup>27</sup> We isolated highly purified CD3<sup>+</sup> T cells, because autoreactive pathogenic and regulatory cells, which potentially play a major role in MS relapse and remission, might be enriched in this fraction. By using 43 DEG as a set of discriminators, hierarchical clustering separated the

cluster of relapse from that of remission. The molecular network of 43 DEG extracted by the common upstream search of KeyMolnet showed the most significant relationship with transcriptional regulation by the nuclear factor-kappa B (NF- $\kappa$ B). NF- $\kappa$ B is a central regulator of innate and adaptive immune responses, cell proliferation, and apoptosis.<sup>28</sup> A considerable number of NF- $\kappa$ B target genes activate NF- $\kappa$ B itself, providing a positive regulatory loop that amplifies and perpetuates inflammatory responses, leading to persistent activation of autoreactive T cells in MS. These observations support the logical hypothesis that NF- $\kappa$ B plays a central role in triggering molecular events in T cells responsible for induction of acute relapse of MS, and suggest that aberrant gene regulation by NF- $\kappa$ B on T-cell transcriptome serves as a molecular biomarker for monitoring the clinical disease activity of MS. Supporting this hypothesis, increasing evidence has shown that NF- $\kappa$ B represents a central molecular target for MS therapy.<sup>29</sup>

We also studied the gene expression profile of purified CD3<sup>+</sup> T cells isolated from four Hungarian monozygotic MS twin pairs with a custom DNA microarray (Hitachi Life Science, Saitama, Japan).<sup>30</sup> By comparing three concordant pairs and one discordant pair, we identified 20 DEG aberrantly regulated between the MS patient and the genetically identical healthy subject. The molecular network of 20 DEG extracted by the common upstream search of KeyMolnet showed the most significant relationship with transcriptional regulation by the Ets transcription factor family. Ets transcription factor proteins, by interacting with various co-regulatory factors, control the expression of a wide range of target genes essential for cell proliferation, differentiation, transformation and apoptosis. Importantly, Ets-1, the prototype of the Ets family members, acts as a negative regulator of Th17 cell differentiation.<sup>31</sup> It is worthy to note that discordant monozygotic MS twin siblings do not show any genetic or epigenetic differences, as validated by whole genome sequencing analysis and genome-scale DNA methylation profiling.<sup>8</sup>

### Biomarkers for predicting IFN $\beta$ responders

Although recombinant IFN $\beta$  therapy is widely used as the gold standard to reduce disease activity of MS, up to 50% of the patients continue to have relapses, followed by progression of disability. If molecular biomarkers for IFN $\beta$  responsiveness are identified, we could use the best treatment options depending on the patients, being invaluable to establish the personalized therapy of MS.

By genome-wide screening of single-nucleotide polymorphisms (SNP) with Affymetrix Human 100K SNP arrays, Byun et al. identified allelic differences between IFN $\beta$  responders and non-responders of RRMS patients in several genes, including HAPLN1, GPC5, COL25A1, CAST and NPAS3, although odds ratios of SNP differences of individual genes are fairly low.<sup>32</sup>

By gene expression profiling with Affymetrix Human Genome U133A Plus 2.0 arrays, Comabella et al. showed that IFN $\beta$  non-responders of RRMS patients after treatment for 2 years are characterized by the overexpression of type I IFN-induced genes in PBMC, associated with increased endogenous production of type I IFN by monocytes at pre-treatment.<sup>33</sup> These observations suggest that a preactivated type I IFN signaling pathway is attributable to IFN $\beta$  non-responsiveness in MS. By gene expression profiling with Affymetrix Human Genome Focus arrays, Sellebjerg et al. showed that *in vivo* injection of IFN $\beta$  rapidly induces elevation of IFI27, CCL2 and CXCL10 in PBMC of MS patients, even after 6 months of treatment,<sup>34</sup> consistent with previous studies.<sup>35</sup> The induction of IFN-responsive genes is greatly reduced in patients with neutralizing antibodies (NABs) against IFN $\beta$ .<sup>34</sup> In contrast, there exist no global differences in gene expression profiles of PBMC of RRMS patients between NABs-negative IFN $\beta$  non-responders and responders.<sup>36</sup>

By gene expression profiling with Affymetrix Human Genome U133A/B arrays, Goertsches et al. found that IFN $\beta$  administration *in vivo* elevates a panel of IFN-responsive genes in PBMC of RRMS patients during a 2-year treatment, but it also down-regulates several genes, including CD20, a known target of B-cell depletion therapy in MS.<sup>37</sup> By using the PATHWAY ARCHITECT software (Stratagene, La Jolla, CA, USA), they identified two major gene networks where upregulation of STAT1 and downregulation of ITGA2B act as a central molecule, although they did not further characterize the responder/non-responder-linked gene expression profiles.

By gene expression profiling with a custom array of the National Institutes of Health (NIH)/National Institute of Neurological Disorders and Stroke (NINDS) Microarray Consortium, Fernald et al. showed that a 1-week IFN $\beta$  administration *in vivo* induces a set of coregulated genes whose networks are related to immune- and apoptosis-regulatory functions, involving JAK-STAT and NF- $\kappa$ B cascades, whereas the networks of untreated subjects are composed of the genes of cellular housekeeping functions.<sup>38</sup> By combining kinetic RT-PCR analysis of

expression of 70 genes in PBMC of RRMS with the integrated Bayesian inference system approach, the same group previously reported that nine sets of gene triplets detected at pretreatment, including a panel of caspases, well predict the response to IFN $\beta$  with up to 86% accuracy.<sup>39</sup>

By gene expression profiling with a custom microarray (Hitachi), we previously identified a set of interferon-responsive genes expressed in purified peripheral blood CD3<sup>+</sup> T cells of RRMS patients receiving IFN $\beta$  treatment.<sup>40</sup> IFN $\beta$  immediately induces a burst of expression of chemokine genes with potential relevance to IFN $\beta$ -related early adverse effects in MS.<sup>41</sup> The majority of the top 30 most significant DEG in CD3<sup>+</sup> T cells between untreated MS patients and healthy subjects are categorized into apoptosis signaling regulators.<sup>42</sup> Furthermore, we found that T cell gene expression profiling classifies a heterogeneous population of Japanese MS patients into four distinct subgroups that differ in the disease activity and therapeutic response to IFN $\beta$ .<sup>43</sup> We identified 286 DEG expressed between 72 untreated Japanese MS patients and 22 age- and sex-matched healthy subjects. By importing the list of 286 DEG into the common upstream search of KeyMolnet, the generated network showed the most significant relationship with transcriptional regulation by NF- $\kappa$ B.<sup>30</sup> Although none of the single genes alone serve as a MS-specific biomarker gene, NR4A2 (NURR1), a target of NF- $\kappa$ B acting as a positive regulator of IL-17 and IFN $\gamma$  production, is highly upregulated in MS T cells.<sup>42,43</sup> It is worthy to note that IFN $\beta$  is beneficial in the disease induced by Th1 cells, but detrimental in the disease mediated by Th17 cells in mouse experimental autoimmune encephalomyelitis (EAE), and IFN $\beta$  non-responders in RRMS patients show higher serum IL-17F levels, suggesting that IL-17 serves as a biomarker predicting a poor IFN $\beta$  response in MS.<sup>44</sup>

#### Molecular networks of MS brain lesion proteome

Recently, Han et al. investigated a comprehensive proteome of six frozen MS brains.<sup>7</sup> Proteins were prepared from small pieces of brain tissues isolated by laser-captured microdissection (LCM), and they were characterized separately by the standard histological examination, and classified into acute plaques (AP), chronic active plaques (CAP) or chronic plaques (CP) based on the disease activity. The proteins were then separated on one-dimensional SDS-PAGE gels, digested in-gel with trypsin, and peptide fragments were processed for mass spectrometric

**Table 1** Multiple sclerosis-linked molecules of the KeyMolnet library

KeyMolnet ID	KeyMolnet symbol	Description
KMMC:04422	2,3cnPDE	2',3'-cyclic nucleotide 3'-phosphodiesterase
KMMC:04421	aBcrystallin	Alpha crystallin B chain
KMMC:01024	ADAM17	A disintegrin and metalloproteinase 17
KMMC:04753	AMPA	AMPA-type glutamate receptor
KMMC:00019	APP	Amyloid beta A4 protein
KMMC:07424	AQP4	Aquaporin 4
KMMC:06672	b-arrestin1	Beta-arrestin 1
KMMC:04017	BAFF	B-cell activating factor
KMMC:00868	Bcl-2	B-cell lymphoma 2
KMMC:00728	Ca	Calcium ion
KMMC:00605	caspase-1	Caspase-1
KMMC:00429	CCL2	Chemokine (C-C motif) ligand 2
KMMC:00425	CCL3	Chemokine (C-C motif) ligand 3
KMMC:00424	CCL5	Chemokine (C-C motif) ligand 5
KMMC:00450	CCR1	Chemokine (C-C motif) receptor 1
KMMC:00454	CCR5	Chemokine (C-C motif) receptor 5
KMMC:03088	CD28	T-cell-specific surface glycoprotein CD28
KMMC:00530	CD80	T-lymphocyte activation antigen CD80
KMMC:03089	CTLA-4	Cytotoxic T-lymphocyte protein 4
KMMC:00418	CXCL10	Chemokine (C-X-C motif) ligand 10
KMMC:00447	CXCR3	Chemokine (C-X-C motif) receptor 3
KMMC:00271	ERa	Estrogen receptor alpha
KMMC:00362	FGF-2	Fibroblast growth factor 2
KMMC:04423	GFAP	Glial fibrillary acidic protein
KMMC:01120	Glu	Glutamic acid
KMMC:00396	glucocorticoid	Glucocorticoid
KMMC:03232	hH1R	Histamine H1 receptor
KMMC:00344	HLA class II	HLA class II histocompatibility antigen
KMMC:09224	HLA-C5	HLA-C5
KMMC:09221	HLA-DQA1*0102	HLA-DQA1*0102
KMMC:06358	HLA-DQA1*0301	HLA-DQA1*0301
KMMC:06359	HLA-DQB1*0302	HLA-DQB1*0302
KMMC:09222	HLA-DQB1*0602	HLA-DQB1*0602
KMMC:06309	HLA-DRB1	HLA-DRB1
KMMC:06315	HLA-DRB1*0301	HLA-DRB1*0301
KMMC:09223	HLA-DRB1*0405	HLA-DRB1*0405
KMMC:09191	HLA-DRB1*11	HLA-DRB1*11
KMMC:07762	HLA-DRB1*15	HLA-DRB1*15
KMMC:06903	HLA-DRB1*1501	HLA-DRB1*1501
KMMC:07763	HLA-DRB1*1503	HLA-DRB1*1503
KMMC:09220	HLA-DRB5*0101	HLA-DRB5*0101
KMMC:04418	HSP105	Heat-shock protein 105 kDa
KMMC:00526	IFNb	Interferon beta
KMMC:00404	IFNg	Interferon gamma
KMMC:00292	IGF1	Insulin-like growth factor 1
KMMC:03611	IgG	Immunoglobulin G
KMMC:00402	IL-10	Interleukin-10
KMMC:03248	IL-12	Interleukin-12
KMMC:04266	IL-12Rb2	Interleukin-12 receptor beta-2 chain
KMMC:03129	IL-17	Interleukin-17
KMMC:03383	IL-18	Interleukin-18
KMMC:00521	IL-1b	Interleukin-1 beta
KMMC:00296	IL-2	Interleukin-2
KMMC:06578	IL-23	Interleukin-23
KMMC:00533	IL-2Rac	Interleukin-2 receptor alpha chain
KMMC:00400	IL-4	Interleukin-4
KMMC:03255	IL-5	Interleukin-5



Table 1 (Continued)

KeyMolnet ID	KeyMolnet symbol	Description
KMMC:00108	IL-6	Interleukin-6
KMMC:03257	IL-7Rac	Interleukin-7 receptor alpha chain
KMMC:00523	IL-9	Interleukin-9
KMMC:00555	iNOS	Inducible nitric oxide synthase
KMMC:00982	int-a4/b1	Integrin alpha-4/beta-1
KMMC:00968	int-aM	Integrin alpha-M
KMMC:00970	int-aX	Integrin alpha-X
KMMC:04094	MBP	Myelin basic protein
KMMC:06533	mGluR	Metabotropic glutamate receptor
KMMC:04420	MOG	Myelin-oligodendrocyte glycoprotein
KMMC:04419	MPLP	Myelin proteolipid protein
KMMC:03210	N-VDCC	Voltage dependent N-type calcium channel
KMMC:04712	NCAM	Neural cell adhesion molecule
KMMC:06537	NCE	Na(+)-Ca <sup>2+</sup> exchanger
KMMC:05576	NeuroF	Neurofilament protein
KMMC:09225	neurofascin	Neurofascin
KMMC:05903	NF-H	Neurofilament triplet H protein
KMMC:05904	NF-L	Neurofilament triplet L protein
KMMC:03785	NMDAR	N-methyl-D-aspartate receptor
KMMC:07764	NMDAR1	N-methyl-D-aspartate receptor subunit NR1
KMMC:07765	NMDAR2C	N-methyl D-aspartate receptor subtype 2C
KMMC:07766	NMDAR3A	N-methyl-D-aspartate receptor subtype NR3A
KMMC:02064	NO	Nitric oxide
KMMC:07767	Olig-1	Oligodendrocyte transcription factor 1
KMMC:01005	OPN	Osteopontin
KMMC:03073	PDGF	Platelet derived growth factor
KMMC:06225	Sema3A	Semaphorin 3A
KMMC:06229	Sema3F	Semaphorin 3F
KMMC:00111	SMAD3	Mothers against decapentaplegic homolog 3
KMMC:03839	tau	Microtubule-associated protein tau
KMMC:00349	TNFa	Tumor necrosis factor alpha
KMMC:00545	VCAM-1	Vascular cell adhesion protein 1
KMMC:03832	VD	Vitamin D
KMMC:03711	VDR	Vitamin D3 receptor

91 multiple sclerosis-linked molecules of the KeyMolnet library are listed in alphabetical order.

analysis. Among 2574 proteins determined with high confidence, the INTERSECT/INTERACT program identified 158, 416 and 236 lesion-specific proteins detected exclusively in AP, CAP and CP, respectively. They found that overproduction of five molecules involved in the coagulation cascade, including tissue factor and protein C inhibitor, plays a central role in molecular events ongoing in CAP. Furthermore, *in vivo* administration of coagulation cascade inhibitors really reduced the clinical severity in EAE, supporting the view that the blockade of the coagulation cascade would be a promising approach for treatment of MS.<sup>43</sup> However, nearly all remaining proteins are uncharacterized in terms of their implications in MS brain lesion development.

We studied molecular networks and pathways of the proteome dataset of Han et al. by using four

different bioinformatics tools for molecular network analysis, such as KEGG, PANTHER, KeyMolnet and IPA.<sup>45</sup> KEGG and PANTHER showed the relevance of extracellular matrix (ECM)-mediated focal adhesion and integrin signaling to CAP and CP proteome. KeyMolnet by the N-points to N-points search disclosed a central role of the complex interaction among diverse cytokine signaling pathways in brain lesion development at all disease stages, as well as a role of integrin signaling in CAP and CP. IPA identified the network constructed with a wide range of ECM components, such as COL1A1, COL1A2, COL6A2, COL6A3, FN1, FBLN2, LAMA1, VTN and HSPG2, as one of the networks highly relevant to CAP proteome. Thus, four distinct tools commonly suggested a role of ECM and integrin signaling in development of chronic

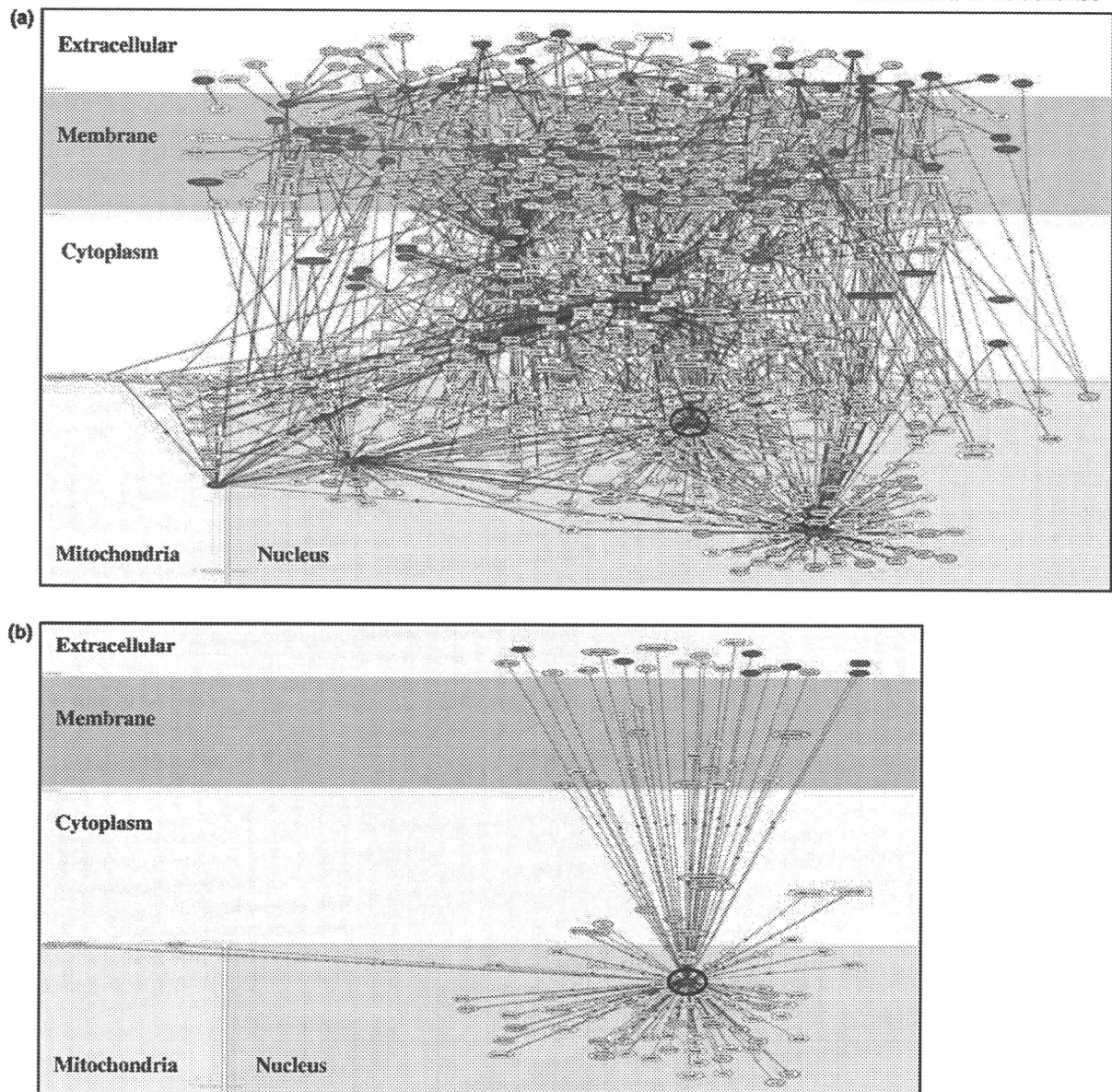


**Figure 2** Molecular network of 91 MS-linked molecules. (a) By importing 91 MS-linked molecules into KeyMolnet, the neighboring search within one path from starting points generates the highly complex molecular network composed of 913 molecules and 1005 molecular relations. (b) The extracted network shows the most significant relationship with transcriptional regulation by vitamin D receptor (VDR) that has direct connections with 118 closely related molecules of the extracted network. VDR is indicated by blue circle. Red nodes represent start point molecules, whereas white nodes show additional molecules extracted automatically from core contents to establish molecular connections. The molecular relation is shown by a solid line with an arrow (direct binding or activation), solid line with an arrow and stop (direct inactivation), solid line without an arrow (complex formation), dash line with an arrow (transcriptional activation), and dash line with an arrow and stop (transcriptional repression). Please refer high resolution figures to URL ([www.my-pharm.ac.jp/~satoj/sub22.html](http://www.my-pharm.ac.jp/~satoj/sub22.html)).

MS lesions, showing that the selective blockade of the interaction between ECM and integrin molecules in brain lesions *in situ* would be a target for therapeutic intervention to terminate ongoing events responsible for the persistence of inflammatory demyelination.

#### KeyMolnet identifies a candidate of molecular targets for MS therapy

The KeyMolnet library includes 91 MS-linked molecules, collected from selected review articles with the highest reliability (Table 1). By importing the list

KeyMolnet ID	KeyMolnet symbol	Description
KMMC:02959	1a,25(OH)2D3	1 alpha, 25-dihydroxyvitamin D3
KMMC:00751	amphiregulin	Amphiregulin
KMMC:03795	ANP	Atrial natriuretic peptide
KMMC:00090	b-catenin	beta-catenin
KMMC:00301	c-Fos	Protooncogene c-fos
KMMC:00183	c-Jun	Protooncogene c-jun
KMMC:00626	c-Myc	Protooncogene c-myc
KMMC:03813	CA-II	Carbonic anhydrase II
KMMC:04105	CalbindinD28K	Vitamin D-dependent calcium-binding protein, avian-type
KMMC:03531	CalbindinD9K	Vitamin D-dependent calcium-binding protein, intestinal
KMMC:00289	caseinK2	Casein kinase 2
KMMC:04195	CaSR	Extracellular calcium-sensing receptor
KMMC:00268	CBP	CREB binding protein
KMMC:00922	CD44	CD44 antigen
KMMC:00136	CDK2	Cyclin dependent kinase 2
KMMC:00135	CDK6	Cyclin dependent kinase 6
KMMC:01008	collagen	Collagen
KMMC:06770	collagenase-I	Type I collagenase
KMMC:04081	CRABP2	Cellular retinoic acid-binding protein II
KMMC:00060	CRT	Calreticulin
KMMC:00401	CXCL8	Chemokine (C-X-C motif) ligand 8 (IL8)
KMMC:00137	cyclinA	Cyclin A
KMMC:00061	cyclinD1	Cyclin D1
KMMC:05926	cyclinD3	Cyclin D3
KMMC:00093	cyclinE	Cyclin E
KMMC:02960	CYP24A1	Cytochrome P450 24A1
KMMC:02958	CYP27B1	Cytochrome P450 27B1
KMMC:04593	CYP3A4	Cytochrome P450 3A4
KMMC:06769	cystatin M	Cystatin M
KMMC:06762	Cytokeratin 13	Keratin, type I cytoskeletal 13
KMMC:06751	Cytokeratin 16	Keratin, type I cytoskeletal 16
KMMC:00053	DHTR	Dihydrotestosterone receptor
KMMC:00928	E-cadherin	E-cadherin
KMMC:00594	ErbB1	Receptor protein-tyrosine kinase erbB-1
KMMC:00068	filamin	Filamin
KMMC:00341	FN1	Fibronectin 1
KMMC:06760	FREAC-1	Forkhead box protein F1
KMMC:06763	G0S2	G0/G1 switch protein 2
KMMC:00617	GM-CSF	Granulocyte macrophage colony stimulating factor
KMMC:06755	Hairless	Hairless protein
KMMC:05978	HOXA10	Homeobox protein Hox-A10
KMMC:06767	HOXB4	Homeobox protein Hox-B4
KMMC:00404	IFNg	Interferon gamma
KMMC:00579	IGF-BP3	Insulin-like growth factor binding protein 3
KMMC:04498	IGF-BP5	Insulin-like growth factor binding protein 5
KMMC:00402	IL-10	Interleukin-10
KMMC:03241	IL-10R	Interleukin-10 receptor
KMMC:03239	IL-10Rac	Interleukin-10 receptor alpha chain
KMMC:03240	IL-10Rbc	Interleukin-10 receptor beta chain
KMMC:03248	IL-12	Interleukin-12
KMMC:03246	IL-12A	Interleukin-12 alpha chain
KMMC:00403	IL-12B	Interleukin-12 beta chain
KMMC:00296	IL-2	Interleukin-2
KMMC:00108	IL-6	Interleukin-6

**Table 2** Molecules constituting the transcriptional regulation by vitamin D receptor network

**Table 2** (Continued)

KeyMolnet ID	KeyMolnet symbol	Description
KMMC:00973	int-b3	Integrin beta-3
KMMC:03747	IVL	Involucrin
KMMC:00629	JunB	Protooncogene jun-B
KMMC:04334	JunD	Protooncogene jun-D
KMMC:06764	KLK10	Kallikrein-10
KMMC:06765	KLK6	Kallikrein-6
KMMC:04635	Mad1	Max dimerization protein 1
KMMC:06757	Metallothionein	Metallothionein
KMMC:06722	MKP-5	MAP kinase phosphatase 5
KMMC:00595	MMP-2	Matrix metalloproteinase 2
KMMC:03104	MMP-3	Matrix metalloproteinase 3
KMMC:00631	MMP-9	Matrix metalloproteinase 9
KMMC:00556	MnSOD	Manganese superoxide dismutase
KMMC:00927	N-cadherin	N-cadherin
KMMC:00074	NCOA1	Nuclear receptor coactivator 1
KMMC:00075	NCOA2	Nuclear receptor coactivator 2
KMMC:00080	NCOA3	Nuclear receptor coactivator 3
KMMC:00282	NCOR1	Nuclear receptor corepressor 1
KMMC:00270	NCOR2	Nuclear receptor corepressor 2
KMMC:00392	NFAT	Nuclear factor of activated T cells
KMMC:00104	NFkB	Nuclear factor kappa B
KMMC:03120	OPG	Osteoprotegerin
KMMC:01005	OPN	Osteopontin
KMMC:00304	osteocalcin	Osteocalcin
KMMC:00100	p21CIP1	Cyclin dependent kinase inhibitor 1
KMMC:00155	p27KIP1	Cyclin dependent kinase inhibitor 1B
KMMC:00195	p300	E1A binding protein p300
KMMC:03204	PLCb1	Phospholipase C beta 1
KMMC:03295	PLCd1	Phospholipase C delta 1
KMMC:00724	PLCg1	Phospholipase C gamma 1
KMMC:04869	plectin1	Plectin 1
KMMC:06772	PMCA1	Plasma membrane calcium-transporting ATPase 1
KMMC:06766	PP1c	Serine/threonine protein phosphatase PP1 catalytic subunit
KMMC:00786	PP2A	Serine/threonine protein phosphatase 2A
KMMC:03442	PPARd	Peroxisome proliferator activated receptor delta
KMMC:03710	PTH	Parathyroid hormone
KMMC:00346	PTHrP	Parathyroid hormone-related protein
KMMC:03115	RANKL	Receptor activator of NFkB ligand
KMMC:04537	RelB	Transcription factor RelB
KMMC:00091	RIP140	Nuclear factor RIP140
KMMC:00383	RXR	Retinoid X receptor
KMMC:06771	SCCA	Squamous cell carcinoma antigen
KMMC:05340	SKIP	Ski-interacting protein
KMMC:04103	SUG1	26S protease regulatory subunit 8
KMMC:05702	TAFII130	Transcription initiation factor TFIID subunit 4
KMMC:06753	TAFII28	Transcription initiation factor TFIID subunit 11
KMMC:06752	TAFII55	Transcription initiation factor TFIID subunit 7
KMMC:04955	TCF-1	T-cell-specific transcription factor 1
KMMC:03075	TCF-4	T-cell-specific transcription factor 4
KMMC:06754	TFIIA	Transcription initiation factor IIA
KMMC:04089	TFIIB	Transcription initiation factor IIB
KMMC:06768	TGase 1	Transglutaminase 1
KMMC:04184	TGFb1	Transforming growth factor beta 1
KMMC:05986	TGFb2	Transforming growth factor beta 2
KMMC:04104	TIF1	Transcription intermediary factor 1
KMMC:00349	TNFa	Tumor necrosis factor alpha



KeyMolnet ID	KeyMolnet symbol	Description
KMMC:00277	TRAP220	Thyroid hormone receptor-associated protein complex component TRAP220
KMMC:06759	TRPV5	TRP vanilloid receptor 5
KMMC:06758	TRPV6	TRP vanilloid receptor 6
KMMC:06756	TRR1	Thioredoxin reductase 1
KMMC:03711	VDR	Vitamin D3 receptor
KMMC:04853	VDUP1	Vitamin D3 up-regulated protein 1
KMMC:06761	ZNF-44	Zinc finger protein 44
KMMC:05147	ZO-1	Tight junction protein ZO-1
KMMC:05811	ZO-2	Tight junction protein ZO-2

Table 2 (Continued)

118 molecules constituting the transcriptional regulation by VDR network are listed in alphabetical order.

of these molecules into KeyMolnet, the neighboring search within one path from starting points generates the highly complex molecular network composed of 913 molecules and 1005 molecular relations (Fig. 2a). The extracted network shows the most significant relationship with transcriptional regulation by vitamin D receptor (VDR) with *P*-value of the score = 4.415E-242. Thus, VDR, a hub that has direct connections with 118 closely related molecules of the extracted network (Fig. 2b, Table 2), serves as one of the most promising molecular target candidates for MS therapy, because the adequate manipulation of the VDR network capable of producing a great impact on the whole network could efficiently disconnect the pathological network of MS. Indeed, vitamin D plays a protective role in MS by activating VDR, a transcription factor that regulates the expression of as many as 500 genes, although the underlying molecular mechanism remains largely unknown.<sup>46</sup>

### Conclusion

MS is a complex disease with remarkable heterogeneity caused by the intricate interplay between various genetic and environmental factors. Recent advances in bioinformatics and systems biology have made major breakthroughs by illustrating the cell-wide map of complex molecular interactions with the aid of the literature-based knowledgebase of molecular pathways. The efficient integration of high-throughput experimental data derived from the disease-affected cells and tissues with underlying molecular networks helps us to characterize the molecular markers and pathways relevant to MS heterogeneity, and promotes us to identify the network-based effective drug targets for personalized therapy of MS.

### Acknowledgements

This work was supported by grants from the Research on Intractable Diseases, the Ministry of Health, Labour and Welfare of Japan (H22-Nanchi-Ippan-136), and the High-Tech Research Center Project, the Ministry of Education, Culture, Sports, Science and Technology (MEXT), Japan (S0801043). The author thanks Dr Takashi Yamamura, Department of Immunology, National Institute of Neurosciences, NCNP for his continuous help with our studies.

### References

- Sospedra M, Martin R. Immunology of multiple sclerosis. *Annu Rev Immunol.* 2005; **23**: 683–747.
- Steinman L. A brief history of T<sub>H</sub>17, the first major revision in the T<sub>H</sub>1/T<sub>H</sub>2 hypothesis of T cell-mediated tissue damage. *Nat Med.* 2007; **13**: 139–45.
- Lucchinetti C, Brück W, Parisi J, Scheithauer B, Rodriguez M, Lassmann H. Heterogeneity of multiple sclerosis lesions: implications for the pathogenesis of demyelination. *Ann Neurol.* 2000; **47**: 707–17.
- Rudick RA, Lee JC, Simon J, Ransohoff RM, Fisher E. Defining interferon  $\beta$  response status in multiple sclerosis patients. *Ann Neurol.* 2004; **56**: 548–55.
- International Multiple Sclerosis Genetics Consortium, Hafler DA, Compston A, Sawcer S, Lander ES, Daly MJ, et al. Risk alleles for multiple sclerosis identified by a genomewide study. *N Engl J Med.* 2007; **357**: 851–62.
- Lock C, Hermans G, Pedotti R, Brendolan A, Schadt E, Garren H, et al. Gene-microarray analysis of multiple sclerosis lesions yields new targets validated in autoimmune encephalomyelitis. *Nature Med.* 2002; **8**: 500–8.
- Han MH, Hwang SI, Roy DB, Lundgren DH, Price JV, Ousman SS, et al. Proteomic analysis of active multiple sclerosis lesions reveals therapeutic targets. *Nature.* 2008; **451**: 1076–81.

8. Baranzini SE, Mudge J, van Velkinburgh JC, Khankhanian P, Khrebtukova I, Miller NA, et al. Genome, epigenome and RNA sequences of monozygotic twins discordant for multiple sclerosis. *Nature*. 2010; **464**: 1351–6.
9. Viswanathan GA, Seto J, Patil S, Nudelman G, Sealfon SC. Getting started in biological pathway construction and analysis. *PLoS Comput Biol*. 2008; **4**: e16.
10. Kitano H. A robustness-based approach to systems-oriented drug design. *Nat Rev Drug Discov*. 2007; **6**: 202–10.
11. Albert R, Jeong H, Barabasi AL. Error and attack tolerance of complex networks. *Nature*. 2000; **406**: 378–82.
12. Satoh J, Tabunoki H, Arima K. Molecular network analysis suggests aberrant CREB-mediated gene regulation in the Alzheimer disease hippocampus. *Dis Markers*. 2009; **27**: 239–52.
13. MAQC Consortium, Shi L, Reid LH, Jones WD, Shippy R, Warrington JA, et al. The MicroArray Quality Control (MAQC) project shows inter- and intraplatform reproducibility of gene expression measurements. *Nat Biotechnol*. 2006; **24**: 1151–61.
14. Huang DW, Sherman BT, Lempicki RA. Systematic and integrative analysis of large gene lists using DAVID bioinformatics resources. *Nat Protoc*. 2009; **4**: 44–57.
15. Subramanian A, Tamayo P, Mootha VK, Mukherjee S, Ebert BL, Gillette MA, et al. Gene set enrichment analysis: a knowledge-based approach for interpreting genome-wide expression profiles. *Proc Natl Acad Sci USA*. 2005; **102**: 15545–50.
16. Kanehisa M, Goto S, Furumichi M, Tanabe M, Hirakawa M. KEGG for representation and analysis of molecular networks involving diseases and drugs. *Nucleic Acids Res*. 2010; **38**: D355–60.
17. Mi H, Dong Q, Muruganujan A, Gaudet P, Lewis S, Thomas PD. PANTHER version 7: improved phylogenetic trees, orthologs and collaboration with the Gene Ontology Consortium. *Nucleic Acids Res*. 2010; **38**: D204–10.
18. Jensen LJ, Kuhn M, Stark M, Chaffron S, Creevey C, Muller J, et al. STRING 8 – a global view on proteins and their functional interactions in 630 organisms. *Nucleic Acids Res*. 2009; **37**: D412–6.
19. Pospisil P, Iyer LK, Adelstein SJ, Kassisi AI. A combined approach to data mining of textual and structured data to identify cancer-related targets. *BMC Bioinformatics*. 2006; **7**: 354.
20. Sato H, Ishida S, Toda K, Matsuda R, Hayashi Y, Shigetaka M, et al. New approaches to mechanism analysis for drug discovery using DNA microarray data combined with KeyMolnet. *Curr Drug Discov Technol*. 2005; **2**: 89–98.
21. Corvol JC, Pelletier D, Henry RG, Caillier SJ, Wang J, Pappas D, et al. Abrogation of T cell quiescence characterizes patients at high risk for multiple sclerosis after the initial neurological event. *Proc Natl Acad Sci USA*. 2008; **105**: 11839–44.
22. Achiron A, Feldman A, Mandel M, Gurevich M. Impaired expression of peripheral blood apoptotic-related gene transcripts in acute multiple sclerosis relapse. *Ann N Y Acad Sci*. 2007; **1107**: 155–67.
23. Gurevich M, Tuller T, Rubinstein U, Or-Bach R, Achiron A. Prediction of acute multiple sclerosis relapses by transcription levels of peripheral blood cells. *BMC Med Genomics*. 2009; **2**: 46.
24. Achiron A, Grotto I, Balicer R, Magalashvili D, Feldman A, Gurevich M. Microarray analysis identifies altered regulation of nuclear receptor family members in the pre-disease state of multiple sclerosis. *Neurobiol Dis*. 2010; **38**: 201–9.
25. Arthur AT, Armati PJ, Bye C; Southern MS Genetics Consortium, Heard RN, Stewart GJ, et al. Genes implicated in multiple sclerosis pathogenesis from compliance of genotyping and expression profiles in relapse and remission. *BMC Med Genet*. 2008; **9**: 17.
26. Brynedal B, Khademi M, Wallström E, Hillert J, Olsson T, Duvefelt K. Gene expression profiling in multiple sclerosis: a disease of the central nervous system, but with relapses triggered in the periphery? *Neurobiol Dis*. 2010; **37**: 613–21.
27. Satoh J, Misawa T, Tabunoki H, Yamamura T. Molecular network analysis of T-cell transcriptome suggests aberrant regulation of gene expression by NF- $\kappa$ B as a biomarker for relapse of multiple sclerosis. *Dis Markers*. 2008; **25**: 27–35.
28. Barnes PJ, Karin M. Nuclear factor- $\kappa$ B. A pivotal transcription factor in chronic inflammatory diseases. *N Engl J Med*. 1997; **336**: 1066–71.
29. Yan J, Greer JM. NF- $\kappa$ B, a potential therapeutic target for the treatment of multiple sclerosis. *CNS Neurol Disord Drug Targets*. 2008; **7**: 536–57.
30. Satoh J, Illes Z, Peterfalvi A, Tabunoki H, Rozsa C, Yamamura T. Aberrant transcriptional regulatory network in T cells of multiple sclerosis. *Neurosci Lett*. 2007; **422**: 30–3.
31. Du C, Liu C, Kang J, Zhao G, Ye Z, Huang S, et al. MicroRNA miR-326 regulates T<sub>H</sub>-17 differentiation and is associated with the pathogenesis of multiple sclerosis. *Nat Immunol*. 2009; **10**: 1252–9.
32. Byun E, Caillier SJ, Montalban X, Villoslada P, Fernández O, Brassat D, et al. Genome-wide pharmacogenomic analysis of the response to interferon beta therapy in multiple sclerosis. *Arch Neurol*. 2008; **65**: 337–44.
33. Comabella M, Lünemann JD, Río J, Sánchez A, López C, Julià E, et al. A type I interferon signature in monocytes is associated with poor response to interferon- $\beta$  in multiple sclerosis. *Brain*. 2009; **132**: 3353–65.
34. Sellebjerg F, Krakauer M, Hesse D, Ryder LP, Alsing I, Jensen PE, et al. Identification of new sensitive biomarkers for the *in vivo* response to interferon- $\beta$  treatment in multiple sclerosis using DNA-array evaluation. *Eur J Neurol*. 2009; **16**: 1291–8.

35. Weinstock-Guttman B, Badgett D, Patrick K, Hartrich L, Santos R, Hall D, et al. Genomic effects of IFN- $\beta$  in multiple sclerosis patients. *J Immunol.* 2003; **171**: 2694–702.
36. Hesse D, Krakauer M, Lund H, Søndergaard HB, Langkilde A, Ryder LP, et al. Breakthrough disease during interferon- $\beta$  therapy in MS: no signs of impaired biologic response. *Neurology.* 2010; **74**: 1455–62.
37. Goertsches RH, Hecker M, Koczan D, Serrano-Fernandez P, Moeller S, Thiesen HJ, et al. Long-term genome-wide blood RNA expression profiles yield novel molecular response candidates for IFN- $\beta$ 1b treatment in relapsing remitting MS. *Pharmacogenomics.* 2010; **11**: 147–61.
38. Fernald GH, Knott S, Pachner A, Caillier SJ, Narayan K, Oksenberg JR, et al. Genome-wide network analysis reveals the global properties of IFN- $\beta$  immediate transcriptional effects in humans. *J Immunol.* 2007; **178**: 5076–85.
39. Baranzini SE, Mousavi P, Rio J, Caillier SJ, Stillman A, Villoslada P, et al. Transcription-based prediction of response to IFN $\beta$  using supervised computational methods. *PLoS Biol.* 2005; **3**: e2.
40. Koike F, Satoh J, Miyake S, Yamamoto T, Kawai M, Kikuchi S, et al. Microarray analysis identifies interferon beta-regulated genes in multiple sclerosis. *J Neuroimmunol.* 2003; **139**: 109–18.
41. Satoh J, Nanri Y, Tabunoki H, Yamamura T. Microarray analysis identifies a set of CXCR3 and CCR2 ligand chemokines as early IFNbeta-responsive genes in peripheral blood lymphocytes in vitro: an implication for IFNbeta-related adverse effects in multiple sclerosis. *BMC Neurol.* 2006; **6**: 18.
42. Satoh J, Nakanishi M, Koike F, Miyake S, Yamamoto T, Kawai M, et al. Microarray analysis identifies an aberrant expression of apoptosis and DNA damage-regulatory genes in multiple sclerosis. *Neurobiol Dis.* 2005; **18**: 537–50.
43. Satoh J, Nakanishi M, Koike F, Onoue H, Aranami T, Yamamoto T, et al. T cell gene expression profiling identifies distinct subgroups of Japanese multiple sclerosis patients. *J Neuroimmunol.* 2006; **174**: 108–18.
44. Axtell RC, de Jong BA, Boniface K, van der Voort LF, Bhat R, De Sarno P, et al. T helper type 1 and 17 cells determine efficacy of interferon- $\beta$  in multiple sclerosis and experimental encephalomyelitis. *Nat Med.* 2010; **16**: 406–12.
45. Satoh JI, Tabunoki H, Yamamura T. Molecular network of the comprehensive multiple sclerosis brain-lesion proteome. *Mult Scler.* 2009; **15**: 531–41.
46. Ascherio A, Munger KL, Simon KC. Vitamin D and multiple sclerosis. *Lancet Neurol.* 2010; **9**: 599–612.

## 基礎 2

# 炎症と T 細胞サブセット

荒浪利昌 山村 隆

あらなみ としまさ, やまむら たかし: 国立精神・神経センター神経研究所 免疫研究部

### ● はじめに

ナイーブ T 細胞は、特異的な抗原に遭遇し活性化されると、特徴的なサイトカインを産生する細胞集団へと分化する。永年にわたって信奉された Th1-Th2 モデルでは、T helper type 1 (Th1) 細胞と Th2 細胞という二極に分化した細胞集団によって、免疫現象の多くが説明されてきた。Th1 細胞はインターロイキン (IL)-12 の存在下で誘導されインターフェロン (IFN)- $\gamma$  を産生する細胞であり、ウイルスなどの細胞内病原体を駆逐する。一方、Th2 細胞は IL-4 の存在下で誘導され、IL-4, IL-5, IL-13 などの Th2 サイトカインの産生を介して、B 細胞増殖、IgE 産生などを誘導し、寄生虫感染の排除において重要な役割を果たす。多発性硬化症 (multiple sclerosis: MS) などの臓器特異的自己免疫疾患では Th1 優位であり、一方、アレルギー疾患は Th2 優位とされてきた。ところが、MS の動物モデルの解析から、IL-17 を産生する T 細胞が病態形成に重要な役割を果たしており、それが Th1 や Th2 細胞とは異なる分化系列に属する細胞であることが証明され、Th17 細胞と名付けられた。本稿では、Th17 細胞を中心に、最近報告された新規 T 細胞サブセットの分化機構および炎症病態における役割を概説する。

### ● Th17 細胞の炎症における役割

IL-17 は 1993 年に活性化 T 細胞において同定されたサイトカインで、現在 IL-17 A から F まで 6 種類のファミリー分子が同定されている。IL-17 A および F が Th17 細胞から産生され、通常単に IL-17 という場合、IL-17 A を指す。IL-17 の生物学的活性は多岐にわたるが、中心的な作用は好中球の活性化と遊走を促進する作用と、TNF- $\alpha$  や MCP-1 などの炎症性サイトカイン/ケモカイン誘導作用である<sup>1)</sup>。このような IL-17 に特徴的な、強力な自然免疫系細胞の動員・活性化作用は、慢性炎症において重要であると考えられる。Th17 細胞は IL-17 以外にも特徴的サイトカインとして、IL-21 や IL-22 を産生する。IL-22 は乾癬病態での働きが示唆されている<sup>2)</sup>。

Th17 細胞が疾患を惹起あるいは増悪させる可能性が、MS、関節リウマチ (RA)、炎症性腸疾患 (IBD)、乾癬や、その動物モデルで報告されている。実際、Th17 細胞の維持や増殖に必須である IL-23 の欠損マウスにおいて、MS や RA の動物モデルは発症せず、Th1 細胞の誘導に必須な IL-12 の欠損マウスでは重篤な病気が起こる<sup>3,4)</sup>。乾癬患者の皮膚では、IL-17 や IL-23 の発現が上昇しており<sup>5)</sup>、IL-12 と IL-23 の共通サブユニットに対する中和抗体は、大規模臨床試験において乾癬症状を有意に抑制し